Preview Control for Vehicle Lateral Guidance in Highway Automation

Huei Peng[1]
Graduate Student Researcher.

Masayoshi Tomizuka
Professor.

Department of Mechanical Engineering,
University of California, Berkeley,
Berkeley, CA 94720

The continuous time deterministic optimal preview control algorithm is applied to the lateral guidance of a vehicle for an automated highway. In the lateral guidance problem, the front wheel steering angle of the vehicle is controlled so that the vehicle follows the center for a lane with small tracking error and maintains good ride quality simultaneously. A preview control algorithm is obtained by minimizing a quadratic performance index which includes terms representing the passenger ride quality as well as the lateral tracking error, each of these terms is multiplied by a frequency dependent weight. This design method is known as a frequency shaped linear quadratic (FSLQ) optimal control approach. It permits incorporating frequency domain design specifications such as high frequency robustness and ride quality in the optimal controller design. It is shown that the optimal preview control law consists of a feedback control term and two feedforward control terms. The feedback term is exactly the same as that of traditional LQ control algorithm. The feedforward preview control action significantly improves the tracking performance and ride quality. Frequency-domain analyses, as well as numerical simulation results, show the improvements achieved by using the preview control algorithm in both the frequency and time domains.

1 Introduction

The lateral control of vehicles is a critical component in highway automation. The objectives are 1) to steer the wheels intelligently so that the vehicle tracks the center of a lane with small error (<20 cm) and 2) to maintain good ride quality under different vehicle speeds, loads, wind gust disturbances, and road surface conditions.

Utilization of information related to the upcoming road characteristics is an important factor in the vehicle lateral control. Roland and Sheridan (1967) stressed the importance of preview information for the human driver, and simulated the drivers' response when the upcoming road suddenly changes. McRuer et al. (1977) proposed that the human driver's control algorithm in performing a regulation task (lane following) consists of two parts: the pursuit (open-loop) block and the compensatory (closed-loop) block. They concluded that the "pursuit" part in the human control system, which previews the future desired path, generates the major part of the driver commands, while the closed-loop portion merely reduces the residue errors. McLean and Hoffmann (1971) conducted spectral analysis on the steering wheel motion of a human driver. The result agrees with McRuer's model, where two peaks occur in the spectral density: a primary peak, which coincides with the dominant frequency of the road being followed, and a secondary peak, which corresponds to the closed-loop compensation motions of the driver. A list of possible visual cues used by human drivers for the pursuit (preview) control action was compiled (McRuer and Weir, 1969); they include the vehicle heading angle (and rate), the vehicle path angle (and rate), and the time-advanced lateral deviation, which is the vehicle displacement at a preview distance. McLean and Hoffmann (1973) performed cross-correlation analysis and suggested that the vehicle heading angle was the dominant variable closely controlled by the human driver under normal driving conditions. When a severely restricted preview length is imposed on the driver the heading rate of the vehicle becomes the major controlled variable.

Godthelp (1986) presented a necessary feedforward steering angle for a particular (step-changed) road curve. This feedforward steering angle gradually ramps up to and down from a steady-state value corresponding to the radius of curvature. Look-ahead vision systems were used to close the feedback loop for automatic guidance of vehicles and mobile robots in many research (Ulmer, 1992; Kenue and Wybo, 1990; Pomerleau, 1992). Future road curvature information is utilized in all these designs implicitly or explicitly.

The optimal preview control for lateral guidance of vehicles has been studied by Lee (1989) from the viewpoint of the discrete time preview control theory (Tomizuka and Rosenthal, 1979; Tomizuka and Whitney, 1975). In this paper, analysis and design of the preview controller is performed in the continuous time domain. In the optimal preview control, the road curvature over a finite preview segment $[t, t + t_{la}]$ is assumed to be known, where t is the present time and t_{la} is the preview time. The road curvature beyond the preview segment is assumed to be nondivergent, and its dynamics are assumed to be known.

[1]Currently with the University of Michigan, Department of Mechanical Engineering and Applied Mechanics, Ann Arbor, MI 48109.

Contributed by the Dynamic Systems and Control Division for publication in the JOURNAL OF DYNAMIC SYSTEMS, MEASUREMENT, AND CONTROL. Manuscript received by the DSCD August 20, 1991; revised manuscript received September 10, 1992. Associate Technical Editor: E. H. Law.

In this paper, the preview control algorithm is incorporated with the frequency-shaped linear quadratic (FSLQ) control theory (Anderson and Moore, 1990; Gupta, 1980), which allows the frequency dependent ride quality to be included in the performance index explicitly. The high-frequency robustness of the control system can be ensured by properly choosing the weighting factors in the performance index.

The road superelevation angle may have significant adverse effects on the lateral control of vehicles if it is not included in the model. We suggest combining the road superelevation angle with the road curvature to form an "effective curvature" for control purposes. The effective curvature replaces the original road curvature in the preview control law, and the preview control law, designed for "curvature only" scenarios, remains unchanged. If the information on superelevation is not available, a large error may occur in the estimation of the average tire cornering stiffness (C_s), which deteriorates the tracking performance of the controller indirectly.

The preview information required for the control algorithm presented in this paper pertains to road curvature and superelevation, which can be measured from the road geometry or obtained from Transportation Agencies. They can be retrieved from an on-board data-base, read from the discrete magnetic reference markers (Zhang et al., 1990), or transmitted from the road to vehicles by a variety of means. Therefore, the present preview control approach is practical to implement.

The remainder of this paper is organized as follows: the continuous time optimal preview control problem is stated in Section 2. In Section 3, a linear vehicle model is presented, and an FSLQ-preview control algorithm is derived. The vehicle lane following problem is formulated as a regulation problem, and the road curvature and superelevation angle are treated as disturbance inputs to the vehicle dynamics. In Section 4, the transfer functions from disturbance (road curvature) to vehicle lateral tracking error and lateral acceleration under preview control are derived. Frequency domain analysis of the preview control algorithm is presented. A numerical simulation study is performed in Section 5 to investigate the response of the vehicle entering curved or superelevated road. The effect of the length of the preview time on the closed-loop response of the vehicle is also studied.

2 Optimal Preview Control Problem

The optimal preview control problems have been studied extensively in the 60's and 70's (Bender, 1968; Oldenberger and Chang, 1965; Sheridan, 1966; Tomizuka, 1976b) in various applications. They can be categorized into two types depending on the "previewed signal": the desired trajectory in a tracking problem, or the external disturbance signal in a regulating problem. Based on the amount of preview information available to the controller, the control problem can be categorized into three types: the feedback control problem, the feedback/feedforward control problem, and the preview control problem. When none of the future information (either desired trajectory or disturbance signal) is available, and the control signal is calculated solely based on the error signal, we have a feedback control problem. When the controller utilizes the current desired trajectory (or disturbance) signal as well as the error signal, it is a feedback/feedforward control problem. When the future information is available and utilized by the control law, we call it a preview control problem. An extensive development of preview control for the tracking problem can be found in (Tomizuka, 1974), and that for the regulation problem can be found in (Tomizuka, 1976a). The optimal preview control algorithm is presented in this paper and applied to the vehicle lateral guidance problem, where the road curvature and superelevation angle enter the system dynamic equation as external disturbances. The following points should be noted:

(1) In this paper, the problem is studied from a deterministic point of view. That is, the road curvature is obtained without any measurement noises, although quantization error may exist.
(2) The preview time is assumed to be finite. In other words, at time t, the road curvature in $\tau \in [t\ t + t_{la}]$ is assumed to be known, where t_{la} is the preview time.

3 Preview Control for Vehicle Lateral Guidance

In the following, a FSLQ preview control problem is developed. Figure 1 shows a schematic diagram of the linear vehicle model used to design the control laws. The system equation for the front-wheel-steered vehicle is (Peng and Tomizuka, 1990):

$$\frac{d}{dt}\begin{bmatrix} y_r \\ \dot{y}_r \\ \epsilon - \epsilon_d \\ \dot{\epsilon} - \dot{\epsilon}_d \end{bmatrix} = \begin{bmatrix} 0 & 1 & 0 & 0 \\ 0 & \frac{A_1}{V} & -A_1 & \frac{A_2}{V} \\ 0 & 0 & 0 & 1 \\ 0 & \frac{A_3}{V} & -A_3 & \frac{A_4}{V} \end{bmatrix} \begin{bmatrix} y_r \\ \dot{y}_r \\ \epsilon - \epsilon_d \\ \dot{\epsilon} - \dot{\epsilon}_d \end{bmatrix} + \begin{bmatrix} 0 \\ B_1 \\ 0 \\ B_2 \end{bmatrix} \delta + \begin{bmatrix} 0 \\ A_2 - V^2 \\ 0 \\ A_4 \end{bmatrix} \frac{1}{\rho}$$

$$\equiv A\mathbf{x} + B\delta + Dw \tag{1}$$

A_i's and B_i's depend on vehicle parameters, and are defined as follows:

$$A_1 = \frac{-2(C_{sf} + C_{sr})}{m} \quad A_4 = \frac{-2(C_{sf} l_1^2 + C_{sr} l_2^2)}{I_z}$$

$$A_2 = \frac{2}{m}(C_{sr} l_2 - C_{sf} l_1) \quad B_1 = \frac{2}{m} C_{sf}$$

$$A_3 = \frac{2}{I_z}(C_{sr} l_2 - C_{sf} l_1) \quad B_2 = \frac{2 l_1 C_{sf}}{I_z} \tag{2}$$

Tire cornering stiffness describes the tire-road interaction and is defined as (Wong, 1978):

$$C_s \equiv \left.\frac{\partial F_y}{\partial \alpha}\right|_{\alpha = 0} \tag{3}$$

Nomenclature

C_{sf} = cornering stiffness of the front tires
C_{sr} = cornering stiffness of the rear tires
d_s = distance from vehicle mass center to the output measurement sensor
I_z = yaw moment of inertia of the vehicle
l_1 = distance from c.g. to the front axle
l_2 = distance from c.g. to the rear axle
m = mass of the vehicle
OXY = inertial coordinate system
V = longitudinal speed of vehicle
w = curvature of the road ($= 1/\rho$)
y_r = lateral distance between the vehicle c.g. and the center line of the road
δ = front wheel steering angle
ϵ = yaw angle of vehicle body
ϵ_d = desired yaw angle set by the road
ρ = radius of curvature of the road

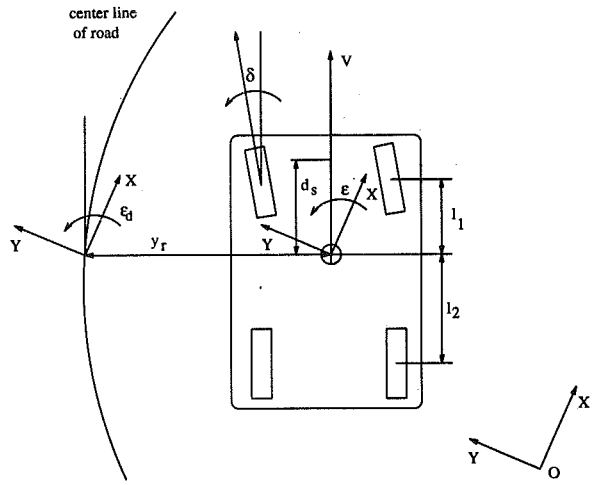

Fig. 1 Schematic diagram of the linear vehicle model

where F_y is the lateral force generated by the tire. α is the tire slip angle, which is the angle between tire orientation and the tire translational speed. The output y_s, taken as the measurement of lateral deviation from a sensor located at a distance d_s ahead of the mass center, can be expressed as:

$$y_s(t) = y_r(t) + d_s(\epsilon(t) - \epsilon_d(t))$$
$$= [1 \;\; 0 \;\; d_s \;\; 0]\mathbf{x}(t) \equiv C\mathbf{x}(t) \quad (4)$$

Specifically, the magnetic marker scheme developed by Zhang (1990) is used for both the simulation study presented in this paper and the experimental work conducted in the PATH program (Peng et al., 1992). In this scheme, magnets are placed along the center of the lane at a fixed spacing. An array of magnetometers are installed at the front end of the vehicle. The vehicle lateral displacement from the lane center is obtained from the magnetic field measurements.

The frequency dependent performance index used for the lateral guidance purposes is:

$$J = \frac{1}{2\pi}\int_{-\infty}^{\infty}\Bigg[a^*(j\omega)\frac{q_a^2}{1+\lambda_a^2\omega^2}a(j\omega) + y_s^*(j\omega)\frac{q_y^2}{1+\lambda_y^2\omega^2}y_s(j\omega) + (\dot\epsilon(j\omega)-\dot\epsilon_d(j\omega))^*\frac{q_\epsilon^2}{1+\lambda_\epsilon^2\omega^2}(\dot\epsilon(j\omega) - \dot\epsilon_d(j\omega)) + y_s^*(j\omega)\frac{q_i^2}{(j\omega)^2}y_s(j\omega) + \delta^*(j\omega)R\delta(j\omega)\Bigg]d\omega \quad (5)$$

where a is the difference between the lateral acceleration of the vehicle mass center $\ddot y_a$ and its desired value V^2/ρ. The coefficients q_a and λ_a are chosen so that the first term of J represents the ride quality. There have been several frequency dependent ride quality standards proposed (e.g., ISO, rms 40, UTACV). They are useful in the selection of λ_a. The coefficients of the next three terms in Eq. (5) are chosen so that the controller reacts to the road curves but is less responsive to the high frequency measurement noises (Peng and Tomizuka, 1990). In this paper, the FSLQ control problem is solved by augmenting the original system, and transforming it into a standard LQ problem following the procedure proposed by Gupta (1990). Define the following augmented state variables:

$$z_1(s) \equiv \frac{q_a}{1+\lambda_a s}a(s) \quad (6)$$

$$z_2(s) \equiv \frac{q_y}{1+\lambda_y s}y_s(s) \quad (7)$$

$$z_3(s) \equiv \frac{q_\epsilon}{1+\lambda_\epsilon s}(\dot\epsilon(s) - \dot\epsilon_d(s)) \quad (8)$$

$$z_4(s) \equiv \frac{q_i}{s}y_s(s) \quad (9)$$

The FSLQ problem is transformed to a standard LQ problem with the following dynamic equation and performance index:

$$\dot{\mathbf{x}}_e(t) = \begin{bmatrix} A & 0 & 0 & 0 & 0 \\ \frac{q_a}{\lambda_a}C_2 & \frac{-1}{\lambda_a} & 0 & 0 & 0 \\ \frac{q_y}{\lambda_y}C & 0 & \frac{-1}{\lambda_y} & 0 & 0 \\ \left[0\;0\;0\;\frac{q_\epsilon}{\lambda_\epsilon}\right] & 0 & 0 & \frac{-1}{\lambda_\epsilon} & 0 \\ q_iC & 0 & 0 & 0 & 0 \end{bmatrix}\mathbf{x}_e(t) + \begin{bmatrix} B \\ \frac{q_aB_1}{\lambda_a} \\ 0 \\ 0 \\ 0 \end{bmatrix}\delta + \begin{bmatrix} D \\ 0 \\ 0 \\ 0 \\ 0 \end{bmatrix}w$$
$$\equiv A_e\mathbf{x}_e(t) + B_e\delta(t) + D_ew(t) \quad (10)$$

$$J(t) = \lim_{t_f\to\infty}\frac{1}{2}\int_t^{t_f}[\mathbf{x}_e^T(\tau)Q\mathbf{x}_e(\tau) + \delta^T(\tau)R\delta(\tau)]d\tau \quad (11)$$

where $\mathbf{x}_e = [\mathbf{x}^T \; z_1 \; z_2 \; z_3 \; z_4]^T$ is the augmented eighth order state vector, A_e, B_e, D_e are the augmented system matrices, $C_2 = [0 \; A_1/V \; -A_1 \; A_2/V]$ is the second row of matrix A, and the weighting matrices Q and R are:

$$Q = \begin{bmatrix} 0&0&0&0&0&0&0&0 \\ 0&0&0&0&0&0&0&0 \\ 0&0&0&0&0&0&0&0 \\ 0&0&0&0&0&0&0&0 \\ 0&0&0&0&1&0&0&0 \\ 0&0&0&0&0&1&0&0 \\ 0&0&0&0&0&0&1&0 \\ 0&0&0&0&0&0&0&1 \end{bmatrix} \quad R = 1 \quad (12)$$

where the weighting coefficients q_a, q_y, q_ϵ, and q_i are absorbed in the augmented state variables, z_i's. It can be shown by Parseval's theorem that the performance index given by Eq. (5) is equivalent to the one in Eq. (11). In the preview FSLQ problem, it is assumed that the disturbance $w(t)$ is previewed with a preview time t_{la}: i.e., $\{w(t+\sigma)\,|\,0 \le \sigma \le t_{la}\}$ is known at time t.

In the following two sections, the optimal preview control laws are developed for two different scenarios. In Section 3.1, the road curvature w is assumed to be available as preview information. In Section 3.2, future information on both road curvature w and superelevation angle γ are assumed to be available.

3.1 Road Curvature Disturbance. Like other linear quad-

ratic optimal control problems, the optimal preview control problem is solved by Dynamic Programming (Bellman, 1957). Recall that the performance index to be minimized is the one in Eq. (11), the following equation can be derived from the principle of optimality:

$$0=\min_{\delta(t)}\left\{\frac{1}{2}\mathbf{x}_e^T(t)Q\mathbf{x}_e(t)+\frac{1}{2}\delta^T(t)R\delta(t)+\frac{dJ^*(t)}{dt}\right\} \quad (13)$$

where $J^*(t)$ is the optimal cost function among all $J(t)$ defined in Eq. (11). The Hamiltonian H is defined to be:

$$H\equiv\frac{1}{2}\mathbf{x}_e^TQ\mathbf{x}_e+\frac{1}{2}\delta^TR\delta+\frac{\partial J^*}{\partial\mathbf{x}_e}(A_e\mathbf{x}_e+B_e\delta+D_ew) \quad (14)$$

The optimal control $\delta_{\text{opt}}(t)$ can then be obtained from:

$$\left.\frac{\partial H}{\partial\delta}\right|_{\delta=\delta_{\text{opt}}}=0 \quad (15)$$

The minimization of the performance index Eq. (11) requires that the disturbance be specified over the problem duration. However, the preview assumption implies that only $\{w(t+\sigma)|0\le\sigma\le t_{la}\}$ is known at time t. A natural way to specify the disturbance beyond the preview segment is to introduce a disturbance generator described by:

$$\frac{dw(\tau)}{d\tau}=A_ww(\tau)\quad \tau\ge t+t_{la} \quad (16)$$

where $A_w\le 0$ governs the decay rate of $w(\tau)$. The optimal preview control algorithm is solved by assuming that the optimal cost function can be expressed by the generalized quadratic form with respect to:

1. The current state vector $\mathbf{x}_e(t)$
2. Disturbance $w(t+\tau)$ in the preview segment $\tau\in[0, t_{la}]$.

The optimal cost function is then expressed as:

$$J^*(\mathbf{x}_e(t),w(t,[0,t_{la}]))=\frac{1}{2}\mathbf{x}_e^T(t)K(t)\mathbf{x}_e(t)+\frac{1}{2}\int_0^{t_{la}}\int_0^{t_{la}}w^T(t,l_1)K_w(t,l_1,l_2)w(t,l_2)dl_1dl_2+\frac{1}{2}w^T(t+t_{la})K_d(t)w(t+t_{la})+\mathbf{x}_e^T(t)\int_0^{t_{la}}F_1(t,l)w(t,l)dl+\mathbf{x}_e^T(t)F_2(t)w(t+t_{la}) \quad (17)$$

where $w(t, l)\equiv w(t+l)$. The optimal control law can be derived from Eqs. (13)-(17):

$$\delta_{\text{opt}}(t)=-R^{-1}B_e^T\left[K(t)\mathbf{x}_e(t)+\int_0^{t_{la}}F_1(t,l)w(t,l)dl+F_2(t)w(t+t_{la})\right] \quad (18)$$

The derivation of Eq. (18) is tedious but straightforward (Peng, 1992). The following equations can be obtained using Eqs. (13)-(18):

$$A_e^TK-KB_eR^{-1}B_e^TK+\dot{K}+KA_e+Q=0$$
$$K(t_f)=0 \quad (19)$$

$$\frac{\partial F_1^T(t,l)}{\partial t}=\frac{\partial F_1^T(t,l)}{\partial l}+F_1^T(t,l)[B_eR^{-1}B_e^TK-A_e]$$
$$F_1^T(t,0)=D_e^TK(t) \quad (20)$$

$$\dot{F}_2^T(t)=F_2^TB_eR^{-1}\mathbf{B}_e^TK-F_1^T(t,t_{la})-F_2^TA_e-A_w^TF_2^T$$
$$F_2(t_f)=0 \quad (21)$$

$$\dot{K}_d(t)=F_2^T(t)B_eR^{-1}\mathbf{B}_e^TF_2(t)-A_w^TK_d(t)$$
$$K_d(t_f)=0 \quad (22)$$

$$\frac{\partial K_w(t,l_1,l_2)}{\partial t}=\frac{\partial K_w(t,l_1,l_2)}{\partial l_1}+\frac{\partial K_w(t,l_1,l_2)}{\partial l_2}+F_1^T(t,l_1)B_eR^{-1}B_e^TF_1(t,l_2)$$
$$K_w(t,t_{la},l)=F_2^T(t)B_eR^{-1}B_e^TF_1(t,l)$$
$$K_w(t,0,l)=D_e^TF_1(t,l) \quad (23)$$

where the boundary conditions of Eqs. (19), (21), and (22) are obtained by comparing Eqs. (11) and (17). It can be seen from Eq. (18) that the optimal control signal only depends on $K(t)$, $F_1(t, l)$ $(0\le l\le t_{la})$ and $F_2(t)$, therefore, Eqs. (22) and (23) are not solved in this paper. However, we would like to point out that both (22) and (23) have proper boundary values and thus can be solved after solving Eqs. (19)-(21). Furthermore, since we are deriving the FSLQ-preview control law, the problem duration is infinite. Therefore, the steady-state solutions of Eqs. (19)-(21) are used.

The preview control law consists of three terms, one feedback term and two feedforward terms. The first term is exactly the same as the feedback control signal in the FSLQ control algorithm, since (19) is the well-known Riccati equation. The second term is the preview action to deal with the disturbance signal within the preview segment. The third term is the preview action to cope with the disturbance beyond the preview segment. Since the feedback part of the preview control algorithm is exactly the same as that of a standard FSLQ controller, the stability of the closed-loop system is guaranteed. The feedforward part of the preview controller further improves the tracking (disturbance rejection) performance by "inverting" the plant dynamics utilizing the future road curvature information.

3.2 Road Superelevation Disturbance. In this section, the road superelevation angle (besides the road curvature) is considered. It is modeled in the system dynamic equation, and its value in the preview segment is assumed to be available. Road superelevation affects not only the lateral tracking performance but also the estimation of the cornering stiffness. If the information on the road superelevation is not available to the controller, a large transient tracking error may occur.

The vehicle lateral dynamic equation, which includes the road superelevation angle γ, is

$$\ddot{y}_r=\frac{\dot{A}_1}{V_r}-A_1(\epsilon-\epsilon_d)+\frac{A_2}{V}(\dot{\epsilon}-\dot{\epsilon}_d)+B_1\delta+\frac{A_2-V^2}{\rho}-g\gamma \quad (24)$$

where g is the gravity constant. It is assumed that the road superelevation angle γ is the same at the front and rear axles of the vehicle. Therefore, the dynamic equation which governs the yaw motion is not affected by γ. Note that γ is assumed to be small so that $\sin\gamma\approx\gamma$ in Eq. (24). There are two approaches to develop the optimal preview control law which handles both the road curvature w and superelevation angle γ:

1 The system dynamic equations can be written as:

$$\dot{\mathbf{x}}_e(t)=A_e\mathbf{x}_e(t)+B_e\delta(t)+[D_{e1}\ D_{e2}]\begin{bmatrix}w(t)\\ \gamma(t)\end{bmatrix} \quad (25)$$

The optimal preview control law can then be obtained by following the procedures described in Section 3.1. Since $D_{e1}\ne D_{e2}$, the road curvature and superelevation must be treated as two exogenous inputs. Therefore, the size of the feedforward gain matrices $F_1(l)$ and F_2 will be doubled.

2 We can incorporate the road curvature information (ρ) and the superelevation information (γ) to form an effec-

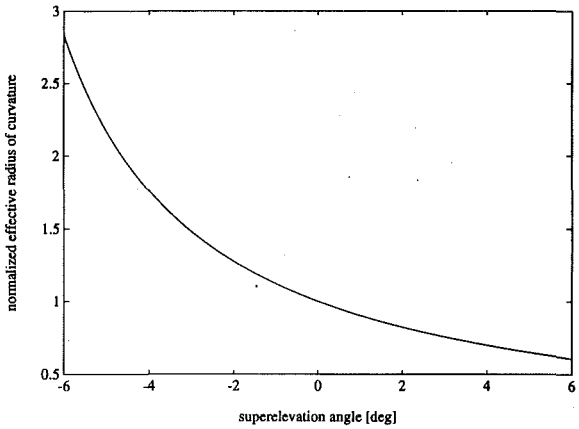

Fig. 2 Normalized effective radius of curvature

tive radius of curvature (ρ'). The preview controller developed in Section 3.1 can then be used to offset the effects due to both the road curvature and the superelevation by substituting ρ with ρ'. It can be seen from Eqs. (1) and (24) that the only difference between the "superelevated" and "nonsuperelevated" dynamic equations is the extra term $-g\gamma$ in Eq. (24). If we define an "effective radius of curvature" (ρ'):

$$\rho' = \frac{A_2 - V^2}{A_2 - V^2 - \rho g \gamma} \times \rho \tag{26}$$

then effects of both road radius and superelevation angle are included. Figure 2 shows the relationship between the normalized effective radius of curvature ρ'/ρ (assuming positive ρ) and road superelevation angle γ. When $\gamma = 0, \rho'/\rho = 1$, and when $\gamma > 0, \rho/\rho' < 1$, the road curvature becomes sharper from the vehicle dynamics point of view.

Notice that in the second approach, it has been implicitly assumed that the effectiveness of preview control is not lost by setting $D_{e1} = D_{e2}$. It will be validated in Section 5 by simulations that the effective radius of curvature ρ' accurately represents the combination of the road superelevation and radius information, from the viewpoints of both feedforward control purposes and tire cornering stiffness estimation purposes. Therefore, the second approach is used in this paper.

3.3 Availability of Road Information. The implementation of preview control algorithm requires future road curvature and superelevation information. These information can be measured from the road or obtained from Transportation Agency easily and accurately. The information can be retrieved from on-board database, obtained through communication link connected to wayside computers, or read from digital coding along the road. Experimental results utilizing a binary coding method have been reported (Peng et al., 1992). If the road geometry information is to be retrieved from an on-board database, the location of the car on the road has to be obtained from other sensing systems (e.g., beacon, global positioning system, etc.).

4 Frequency Domain Analysis

By using the steady-state gains of K, F_1, and F_2, the effect of the preview control can be interpreted from the viewpoint of frequency domain analysis. The steady-state solution (K_{ss}) of Eq. (19) is obtained from the Algebraic Riccati Equation (ARE), and the steady-state solutions of F_1 and F_2 are

$$F_1(l) = e^{A_c^T l} K_{ss} D_e \tag{27}$$

$$F_2 = -(A_c^T + A_w I)^{-1} e^{A_c^T t_{la}} K_{ss} D_e \tag{28}$$

respectively, where $A_c \equiv A_e - B_e R^{-1} B_e^T K_{ss}$ is the closed-loop system matrix. It should be noted that:

(1) The feedforward gains $F_1(l)$ and F_2 are functions of the feedback gain K_{ss}.
(2) Equation (28) is no longer true if there is more than one disturbance signal in this system. No closed-form solution of F_2 exists when there are multiple disturbance signals.

Substituting (27) and (28) into (18), we obtain:

$$\begin{aligned}\delta_{\text{opt}}(s) &= -R^{-1}B_e^T\Big[K_{ss}\mathbf{x}_e(s) + \int_0^{t_{la}} F_1(l)e^{ls}dl\,w(s) + F_2 e^{t_{la}s}w(s)\Big] \\ &= -R^{-1}B_e^T\Big[K_{ss}\mathbf{x}_e(s) + \int_0^{t_{la}} e^{A_c^T l}K_{ss}D_e e^{ls}dl\,w(s) \\ &\quad - (A_c^T + A_w I)^{-1}e^{A_c^T t_{la}}K_{ss}D_e e^{t_{la}s}w(s)\Big]\end{aligned} \tag{29}$$

To simplify Eq. (29), we note the following relation:

$$\begin{aligned}\int_0^{t_{la}} e^{A_c^T l}e^{ls}dl &= \frac{1}{s}e^{A_c^T l}e^{ls}\Big|_0^{t_{la}} - \int_0^{t_{la}}\frac{1}{s}A_c^T e^{A_c^T l}e^{ls}dl \\ &= \frac{1}{s}(e^{A_c^T t_{la}}e^{t_{la}s} - I) - \frac{1}{s}A_c^T\int_0^{t_{la}} e^{A_c^T l}e^{ls}dl\end{aligned} \tag{30}$$

or

$$\int_0^{t_{la}} e^{A_c^T l}e^{ls}dl = (sI + A_c^T)^{-1}(e^{A_c^T t_{la}}e^{t_{la}s} - I) \tag{31}$$

Substituting (31) into (29), we have:

$$\begin{aligned}\delta_{\text{opt}}(s) &= -R^{-1}B_e^T K_{ss}\mathbf{x}_e(s) - R^{-1}B_e^T(sI + A_c^T)^{-1} \\ &\quad \times (e^{A_c^T t_{la}}e^{t_{la}s} - I) - K_{ss}D_e w(s) + R^{-1}B_e^T \\ &\quad \times (A_c^T + A_w I)^{-1}e^{A_c^T t_{la}}K_{ss}D_e e^{t_{la}s}w(s)\end{aligned} \tag{32}$$

From Eqs. (32) and (10), the transfer function from road curvature w to tracking error y_s is:

$$\begin{aligned}G_y(s) &= c_e(sI - A_c)^{-1}[D_e - B_e R^{-1}B_e^T(sI + A_c^T)^{-1} \\ &\quad \times (e^{A_c^T t_{la}}e^{t_{la}s} - I)K_{ss}D_e + B_e R^{-1}B_e^T(A_c^T + A_w I)^{-1} \\ &\quad \times e^{A_c^T t_{la}}K_{ss}\mathbf{D}_e e^{t_{la}s}]\end{aligned} \tag{33}$$

where $c_e = [1\ 0\ d_s\ 0\ 0\ 0\ 0\ 0]$ is the FSLQ-augmented output matrix.

To investigate the effect of preview control on ride quality, the transfer function from w to lateral acceleration $\ddot{y}_a$ is also derived. Note that the total lateral acceleration can be computed from:

$$\begin{aligned}\ddot{y}_a &\approx \ddot{y}_r + \frac{V^2}{\rho} = C_{acc}\mathbf{x}_e + B_1\delta + D_1 w + \frac{V^2}{\rho} \\ &= C_{acc}\mathbf{x}_e + B_1\delta + D_1 w + V^2 w\end{aligned} \tag{34}$$

where $c_{acc} = [0\ A_1/V\ -A_1\ A_2/V\ 0\ 0\ 0\ 0]$ is the lateral acceleration output matrix. Substituting (32) into (34), the transfer function from road curvature w to lateral acceleration $\ddot{y}_a$ is obtained:

$$\begin{aligned}G_a(s) &= (c_{acc} - B_1 R^{-1}B_e^T K_{ss})(sI - A_c)^{-1} \\ &\quad \times [D_e - B_e R^{-1}B_e^T(sI + A_c^T)^{-1}(e^{A_c^T t_{la}}e^{t_{la}s} - I)K_{ss}D_e \\ &\quad + B_e R^{-1}B_e^T(A_c^T + A_w I)^{-1}e^{A_c^T t_{la}}K_{ss}\mathbf{D}_e e^{t_{la}s}] \\ &\quad + B_1[-R^{-1}B_e^T(sI + A_c^T)^{-1}(e^{A_c^T t_{la}}e^{t_{la}s} - I)K_{ss}D_e \\ &\quad + R^{-1}B_e^T(A_c^T + A_w I)^{-1}e^{A_c^T t_{la}}K_{ss}\mathbf{D}_e e^{t_{la}s}] + \mathrm{A}_2\end{aligned} \tag{35}$$

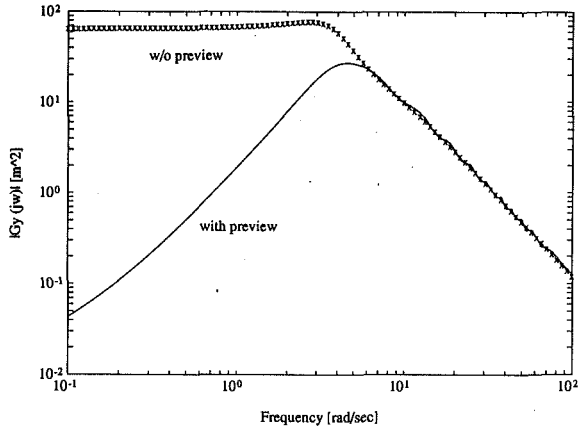

Fig. 3 Frequency response of $G_y(s)$

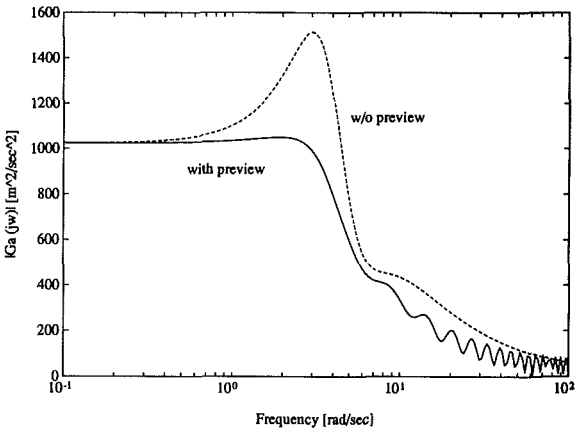

Fig. 4 Frequency response of $G_a(s)$

The transfer functions $G_y(s)$ and $G_a(s)$ are plotted in Figs. 3 and 4, respectively, for the nominal system parameters listed in Table 1. Two cases are plotted in each figure: with preview (t_{la} = 1.0 s) and without preview (t_{la} = 0). It can be seen that the preview control signal improves both the tracking error in the low frequency region and the lateral acceleration in the high frequency region. The following points should be noted:

(1) The preview controller improves the low-frequency tracking performance up to a certain frequency, beyond which (when the road curvature changes faster) there is no improvement at all. This frequency was found to be the closed-loop cut-off frequency of the transfer function (G_s) between steering input δ and tracking error y_s (see Fig. 5).

(2) Preview control reduces the lateral acceleration between 1 and 80 rad/s. At low frequency, the lateral acceleration is governed by the relation $\ddot{y}_a = V^2/\rho$, and cannot be reduced by preview actions. The magnitude of $G_a(j\omega)$ approaches V^2 as frequency approaches zero for both previewed and un-previewed cases.

5 Simulation Results

In the following, the simulations are performed on a complex vehicle model, which includes all the six degree-of-freedom motions of the vehicle sprung mass, plus a nonlinear tire and suspension model (Peng, 1992). This model has been validated by experimental data (Peng et al., 1992), and was found to predict the response of the vehicle more accurately than the linear vehicle model presented in Section 3. The hypothetical test track used in the simulations consists of a curved section connecting two straight sections. The parameter utilized in the simulations are the nominal values listed in Table 1, unless otherwised stated. A first-order time-lag model with a 150 ms time constant is used to describe the steering actuator dynamics. The sampling time for measurement and control is assumed to be 10 ms. The lateral tracking error is assumed to be obtained intermittently from discrete markers on the road center. The discrete markers are assumed to be placed at 1.0 meter spacing, which determines not only the measurement rate of the tracking error, but also the updating rate of the preview (curvature and superelevation) information. The average tire cornering stiffness (C_s) is estimated based on the vehicle dynamics Eqs. (1) for gain scheduling purposes (Peng and Tomizuka, 1990).

Table 1 Simulation parameters

Symbol	meaning	value
m (kg)	mass	1573
I_z (kg – m^2)	mom. of iner.(z)	2783
C_{sf} (N/rad)	front cor. stiff.	46000
C_{sr} (N/rad)	rear cor. stiff.	37800
V (m/s)	vehicle speed	32
ρ (m)	radius of curve	630
l_1 (m)	dist. c.g. to front axle	1.034
l_2 (m)	dist. c.g. to rear axle	1.491
d_s (m)	dist. c.g. to magnetometers	1.9
T_s (s)	sampling time	0.01
D_m (m)	marker spacing	1.0
t_{la} (s)	preview time	1.0
A_w	dist. decay rate	0

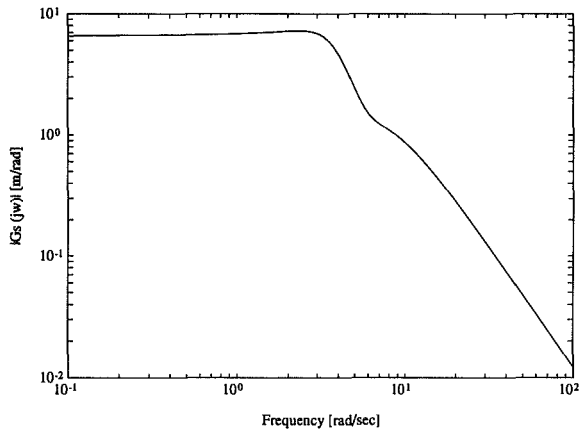

Fig. 5 Frequency response of $G_s(s)$

A_w in the disturbance dynamics (16) is chosen to be zero. In other words, the road curvature is assumed to be unchanged beyond the preview segment $[t, t + t_{la}]$. Furthermore, to implement the preview control law in real-time, a summation is used to approximate the integration term in (18). The values of λ_a, λ_y, and λ_ϵ are 0.0053, 0.23, and 0.23, respectively.

Nominal Case. Figure 6 shows the simulation results when the vehicle is steered by the preview control law. The response of the vehicle controlled by the FSLQ feedback plus steady-state feedforward control law is presented for comparison, in which case the steady-state steering angle corresponding to the current road curvature is added to the feedback control signal. The vehicle, with initial tracking error of 10 cm, is following a straight section of the road from t = 0 to t = 3 s. A curve of 630 m radius presents between t = 3 to t = 7 s. Finally, the road is assumed to be straight after t = 7 s. It can be seen from the initial error response that the feedback part of the controllers are the same in these two cases. However, the preview control algorithm foresees the change in road curvature, and initiates steering action before the vehicle enters and leaves the curved section. Therefore, the overshoot in tracking error when the vehicle enters the curve is much smaller than the case

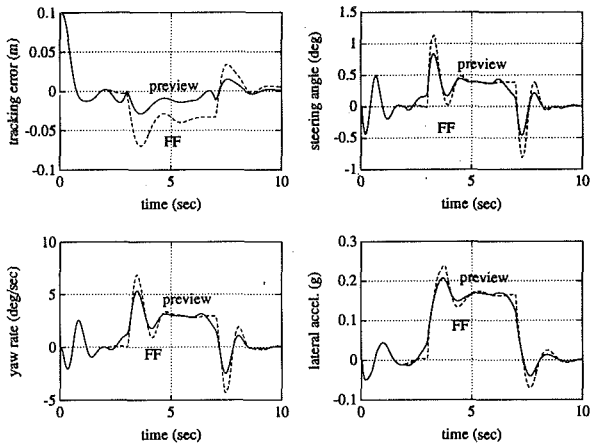

Fig. 6 Simulation of vehicle lateral control system (preview versus FF)

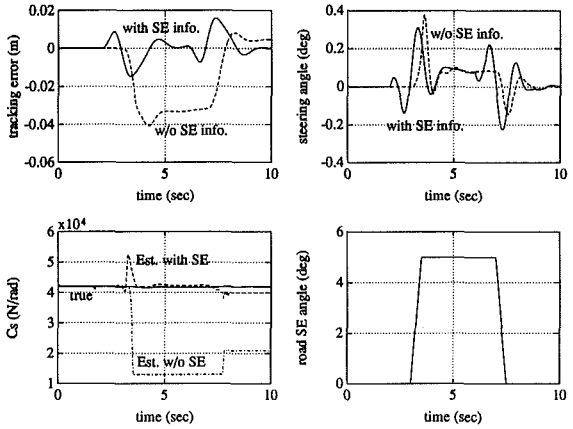

Fig. 7 Simulation of vehicle lateral control system (superelevated road)

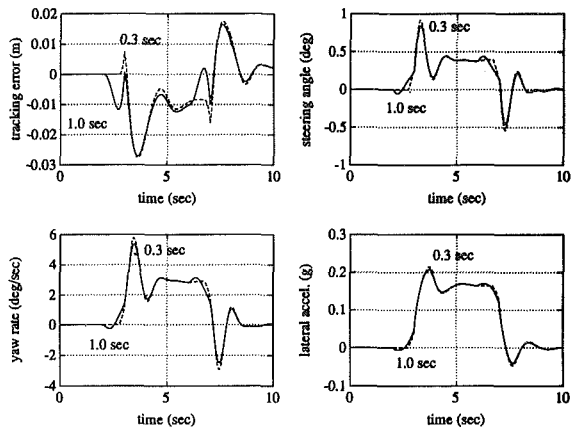

Fig. 8 Simulation of vehicle lateral control system (variable t_{la})

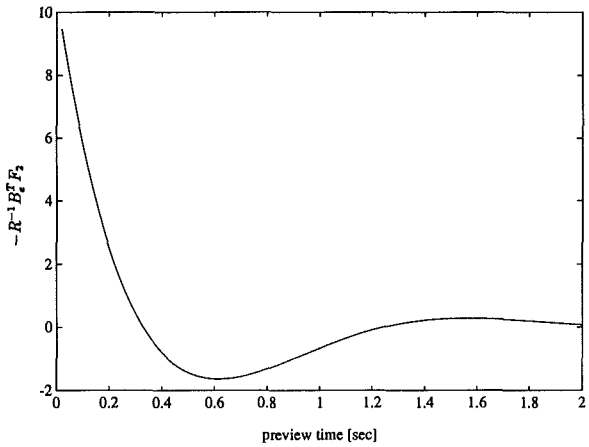

Fig. 9 $-R^{-1}B_e^TF_2$ as function of preview time t_{la}

with steady-state feedforward controller. Furthermore, since the controller has a longer time to respond to the sudden change in road curvature, the peak steering angle as well as vehicle lateral acceleration and yaw rate are also reduced. In other words, the passenger ride quality is also improved by applying the preview control algorithm.

Road Superelevation. Figure 7 shows the results of the vehicle driving on a straight but superelevated road. Two sets of results are presented. In the first run, the effective radius of curvature ρ' is used (which includes the superelevation (SE) information). In the second run, the original road radius of curvature is used. In other words, the road superelevation information is used in the first run but not in the second run. It can be seen that a large error occurs in the estimation of C_s in the second run, and the tracking performance deteriorates noticeably. When the road SE information is utilized, both the steady-state tracking error and the maximum steering angle in the curved section are smaller than those of the case when the road SE information is not used.

Variable t_{la}. Figure 8 shows the response of the vehicle under preview control of different preview time t_{la}. The vehicle is assumed to drive on the same test track described in the nominal case simulation. It can be seen that when t_{la} is 0.3 s, peak values of both tracking error and lateral acceleration are about the same as those corresponding to longer t_{la}, even though the steering action is initiated later. When t_{la} is long (1 second), reverse action appears when the vehicle enters (and leaves) the curve. In other words, the vehicle is steered to the opposite direction from the curve, and then back to the correct direction. The reverse action disappears when the preview time is short ($t_{la} = 0.3$ second). It can be seen from Eq. (18) that the reverse action occurs when $-R^{-1}B_e^TF_2$ is negative. Figure 9 shows the value of $-R^{-1}B_e^TF_2$ as t_{la} varies. Reverse action occurs whenever t_{la} is greater than 0.32 second, and reaches its peak value at around $t_{la} = 0.6$ second.

6 Conclusions

The preview control design procedure is combined with the Frequency Shaped Linear Quadratic (FLSQ) control design method. The resulting preview controller can be decomposed into a feedback part and a feedforward part. The feedback part is exactly the same as that of FSLQ controller. Therefore, the advantages of FSLQ feedback control approach (see Gupta, 1980 for example) are preserved. The tracking (disturbance rejection) performance of the closed-loop system is further improved by the feedforward part, which "inverts" the plant dynamics by utilizing the future desired trajectory (or disturbance) information. This design procedure is applied to the vehicle lateral guidance problem in this paper. The effectiveness of the preview control design procedure is evaluated in both time and frequency domains. Results of the frequency-domain analysis show that the preview control law improves the low frequency tracking performance and reduces high frequency lateral acceleration simultaneously. Results from the numerical simulation study confirm that the preview control algorithm improves the tracking performance as well as passenger ride quality when the vehicle enters/leaves curved or superelevated sections. Experimental results show that the test vehicle could not track the magnetic reference without preview. Details of the experiments will be presented in future publications.

Acknowledgments

The research reported herein is supported by the Parters for Advanced Transit and Highways (PATH) program, performed under the sponsorship of the State of California Business, Transportation, and Housing Agency, Department of Transportation, and the U.S. Department of Transportation, Federal Highway Administration.

References

Anderson, B., and Moore, J., 1990, *Optimal Control—Linear Quadratic Methods*, Prentice Hall.

Bellman, R. E., 1957, *Dynamic Programming*, Princeton University Press.

Bender, E. K., 1968, "Optimum Linear Preview Control With Application to Vehicle Suspension," ASME *Journal of Basic Engineering*, pp. 213–221.

Godthelp, H., 1986, "Vehicle Control During Curve Driving," *Human Factors*, Vol. 28.

Gupta, N., 1980, "Frequency-Shaped Cost Functionals: Extension of Linear-Quadratic-Gaussian Design Methods," *Journal of Guidance and Control*, Vol. 3, pp. 529–535.

Kenue, S. K., and Wybo, D. R., 1990, "Lanelok: An Improved Hough Transform Algorithm for Lane Sensing Using Strategic Search Method," Technical report, GMR report-7157.

Lee, A. Y., 1989, "A Preview Steering Autopilot Control Algorithm for Four-Wheel-Steering Passenger Vehicles," *Advanced Automotive Technologies*, pp. 83–98.

McLean, J. R., and Hoffmann, E. R., 1971, "Analysis of Drivers' Control Movements," *Human Factors*, Vol. 13, pp. 407–418.

McLean, J. R., and Hoffmann, E. R., 1973, "The Effects of Restricted Preview on Driver Steering Control and Performance," *Human Factors*, Vol. 15.

McRuer, D. T., Allen, R. W., Weir, D. H., and Klein, R. H., 1977, "New Results in Driver Steering Control Models," *Human Factors*, Vol. 19.

McRuer, D. T., and Weir, D. H., 1969, "Theory of Manual Vehicular Control," *Ergonomics*, Vol. 12.

Oldenberger, R., and Chang, R., 1965, "Optimal Nonlinear Control for Step and Pulse Disturbances," ASME *Journal of Basic Engineering*, Vol. 87, pp. 319–325.

Peng, H., 1992, "Vehicle Lateral Control for Highway Automation," Ph.D. dissertation, UC Berkeley.

Peng, H., et al., 1992, "A Theoretical and Experimental Study on Vehicle Lateral Control," *Proceedings of American Control Conference*.

Peng, H., and Tomizuka, M., 1990, "Lateral Control of Front-Wheel-Steering Rubber-Tire Vehicles," Technical report, PATH program, ITS, UC Berkeley.

Pomerleau, D., 1992, "Neural Network Perception for Mobile Robot Guidance," PhD thesis, Carnegie-Mellon University.

Roland, R. D., and Sheridan, T. B., 1967, "Simulation Study of the Driver's Control of Sudden Changes in Previewed Path," MIT, Dept. of Mech. Eng., Report DSR 74920-1.

Sheridan, T., 1966, "Three Models of Preview Control," *IEEE Trans. on Human Factors in Electronics*, Vol. 7.

Tomizuka, M., 1974, "The Optimal Finite Preview Problem and Its Application to Man-Machine Systems," Ph.D. dissertation, M.I.T.

Tomizuka, M., 1976a, "The Continuous Optimal Finite Preview Control Problem," *Trans. of the Society of Instrument and Control Engineers*, Vol. 12, pp. 7–12 (in Japanese).

Tomizuka, M., 1976b, "Optimum Linear Preview Control with Application to Vehicle Suspension—Revisited," ASME JOURNAL OF DYNAMIC SYSTEMS, MEASUREMENT, AND CONTROL, pp. 309–315.

Tomizuka, M., and Rosenthal, D. E., 1979, "On the Optimal Digital State Vector Feedback Controller with Integral and Preview Actions," *Trans. ASME*, Vol. 101, pp. 172–178.

Tomizuka, M., and Whitney, D. E., 1975, "Optimal Discrete Finite Preview Problems (Why and How is Future Information Important?)," ASME JOURNAL OF DYNAMIC SYSTEMS, MEASUREMENT, AND CONTROL, pp. 319–325.

Ulmer, B., 1992, "Vita—An Automous Road Vehicle (arv) for Collision Avoidance in Traffic," *Intelligent Vehicle 1992*.

Wong, J. Y., 1978, *Theory of Ground Vehicle*, John Wiley & Sons.

Zhang, W., Parsons, R., and West, T., 1990, "An Intelligent Roadway Reference System for Vehicle Lateral Guidance Control," *Proceedings of American Control Conference*.